

## Estimate of the climatic and environmental variability in Italy in the last Millennia

As previously reported in the IPCC report 2007, the last two millennia represent an important time interval for testing the past climate oscillations and for the determination of the reliability of medium and long-term prediction models. In addition, this short time interval allows comparison of data from historical documents, instrumental and paleodata records with multi-decadal-to-centennial variability arising from external forcing and internal climate variability (IPCC, 2013 and 2014). Previous studies have documented, during this time interval, the occurrence of considerable climate oscillations of significant amplitude and duration that played an important role in social reorganizations in Europe. Anyway, our understanding of the magnitude and spatial extent as well as the possible causes and concurrences of climate changes during this period are still limited and the scarcity of integrated information from marine records emerges. In this framework, the Mediterranean area is considered one of the climatically highly sensitive regions (hotspot) to global change and due to its paleo-latitudinal and land locked configuration, is an ideal archive to investigate paleoclimate changes at secular scale. The goal of these this Challenge (Italy-2k) is to provide information on the climatology and climate variability in Italy in the last two thousand years, by a blend of paleoclimatic data information (ice and sediment cores, pollens, peat bog data, dendroclimatology) and numerical simulations. Station data, numerical simulations and marine reconstructions/reanalyses will allow for a more detailed representation of climate variability in the last 100 years.

### Marine sedimentary archives

One of the main result obtained from comparison of marine fossil archives of the Mediterranean basin (including surrounding area of Italian peninsula) is the chronologically correspondence of the principal observed changes with the historical climatic phases defined in literature (Tab. 1), which match to the major cultural and social reorganization of the Mediterranean region (Lirer et al., 2014; Margaritelli et al., 2016, 2018; Cisneros et al., 2016; Di Rita et al., 2018; Jalali et al., 2018; Cascella et al., accepted), with a consequent possible anthropogenic impact on marine ecosystems.

Nieto Moreno et al. (2011)		Nieto Moreno et al. (2012)		Margaritelli et al. (2018)		Jalali et al. (2018)		Margaritelli et al. (2016)		Lirer et al. (2014)		Gruzel et al. (2013)		Goudeau et al. (2012)		Flux et al. (2008)		Gogou et al. (2014)	
west Algerian-Balearic basin		western Aegean Sea		Misraia basin		Gulf of Lion		central Tyrrhenian Sea		south Tyrrhenian Sea		Ionian Sea		Ionian Sea		Adriatic Sea		Aegean Sea	
Climatic phase	Age	Climatic phase	Age	Climatic phase	Age	Climatic phase	Age	Climatic phase	Age	Climatic phase	Age	Climatic phase	Age	Climatic phase	Age	Climatic phase	Age	Climatic phase	Age
								Modern Warm Period	upwards-1950 AD	Modern Warm Period	2040 AD - upwards			Present	1894 AD - 1958 AD				
		Industrial Period	1800 AD - upwards	Industrial Period	1850 AD - upwards	Industrial Period	1850 AD - upwards	Industrial Period	1850 AD - upwards	Industrial Period	1940 AD - upwards								
Little ice Age	1800 AD - 1300 AD	Little ice Age	1800 AD - 1300 AD	Little ice Age	1850 AD - 1200 AD	Little ice Age	1850 AD - 1400 AD	Little ice Age	1850 AD - 1250 AD	Little ice Age	1850 AD - 1240 AD	Little ice Age	1850 AD - 1400 AD	Little ice Age	1850 AD - 1400 AD	Little ice Age	1840 AD - 1400 AD	Little ice Age	1850 AD - 1300 AD
Medieval Classic Anomaly	1300 AD - 800 AD	Medieval Classic Anomaly	1300 AD - 800 AD	Medieval Climate Anomaly	1200 AD - 850 AD	Medieval Climate Anomaly	1400 AD - 900 AD	Medieval Climate Anomaly	1200 AD - 800 AD	Medieval Classic Anomaly	1240 AD - 840 AD	Medieval Warm Period	1200 AD - 800 AD	Medieval Classic Anomaly	1200 AD - 800 AD	Medieval Warm Period	1200 AD - 800 AD	Medieval Warm Period	1300 AD - 900 AD
Dark Age	800 AD - 500 AD	Dark Age	800 AD - 500 AD	Dark Age	850 AD - 500 AD	Dark Age Cold Period	800 AD - 200 AD	Dark Age	800 AD - 550 AD	Dark Age	840 AD - 550 AD	Dark Age	750 AD - 500 AD			Dark Age	600 AD - 350 AD	Dark Age	900 AD - 500 AD
Roman Warm Period	50 AD - 450 BC	Roman Warm Period	500 AD - 450 BC	Roman Warm Period	500 AD - 50 BC	Roman period	200 AD - 500 BC	Roman period	550 AD - 500 BC	Roman period	500 AD - 500 BC	Roman Warm Period	500 AD - 100 AD	Roman Warm Period	450 BC - 0 AD	Roman Warm Period	550 AD - 100 BC	Roman Warm Period	500 AD - 0 AD

Tab. 1. Table with ages and nomenclature of the climatic events documented in marine Mediterranean records for the last two millennia

For the first time, Margaritelli et al. (2018) provided an oxygen stable isotope ( $\delta^{18}\text{O}$  *Globigerinoides ruber* records) regional scale correlation of different Mediterranean areas over the last ca. 2000 years of Common Era (CE). This correlation, notwithstanding differences in resolution and age model, allowed to underline a general good agreement between the long and short term climate oscillations documented in sea surface Mediterranean  $\delta^{18}\text{O}$  signatures, over the last two millennia (Fig. 2). Al almost synchronicity of the identified short term events suggest an homogeneous response of marine system to climate oscillation and represent a robust framework to better understand global forcing within the Mediterranean region. In addition, the comparison of the marine signals with north European continental ones, allows to highlight a similar climate evolution at Mediterranean scale. The Roman Period and in particular the so-called "Roman Climatic Optimum" covers the time interval from ca. 1 CE to ca. 500 CE (Fig. 2). This phase is characterized by prosperity and expansion of the civilizations and it could represent a possible paleo analogue of the modern warm climate condition

in the Mediterranean area. This warming phase is documented in the Sea Surface Temperature (SST) reconstruction in the Alboran Sea (Rodrigo-Gamiz et al., 2014), Minorca basin (Cisneros et al., 2016), Sicily channel (Margaritelli et al., submitted) and in the Aegean Sea (Katsouras, 2009; Kontakiotis 2016). Stable isotope *G. ruber* signatures show that the Roman Period is also punctuated by three short term cooling events (Roman I, II and III) those chronologically correspond to solar minima activity (Lirer et al., 2014; Margaritelli et al., 2016, 2018) (Fig. 2). In particular, the Roman III cold event falls very close to the 476 CE when historically is documented the fall of Western Roman Empire. In addition, the observed correspondence between the cold Roman III event with the north hemisphere continental temperature anomaly reveal a remarkable connection between continental and marine climatic pattern (Fig. 2).

After the Fall of the Roman Empire, heavy values in  $\delta^{18}\text{O}_{\text{G.ruber}}$  records support an amelioration of the regional climate condition at the base of the Dark Age (ca. 550 to 700 CE) (Fig. 2). This climate phase, coincident with the wetter phase documented in lake sediment of Sicily, results almost coincident with the Justinian Plague (541-749 CE). Upwards, according to Margaritelli et al. (2018), a prominent cooling event in the upper part of Dark Age, also documented in the north Europe continental records, and corresponding to the Roman IV solar minimum, marks the beginning of a long term cooling trend (spanning ca. the following 1100 yr) that culminates during the Little Ice Age (Fig. 2).

The Medieval Climate Anomaly (MCA) was characterized by rather temperate (Lirer et al., 2014; Cisneros et al., 2016; Margaritelli et al., 2016, 2018) and probably more arid climate conditions. Heavy values in  $\delta^{18}\text{O}_{\text{G.ruber}}$  Mediterranean records in the lower part of the MCA result almost in phase with the north Hemisphere positive temperature anomaly, confirming the amelioration of the regional scale climate condition (Fig. 2). Later, between ca. 1050-1100 CE, Margaritelli et al. (2016, 2018) documented a short - term cold dry event, termed Medieval Cold Event (MCE), in  $\delta^{18}\text{O}_{\text{G.ruber}}$  Mediterranean records, also associated with a decrease in arboreal vegetation (Margaritelli et al., 2016; Di Rita et al., 2018, 2018a) suggesting more arid climate condition (Fig. 2). The MCA ends with a short – term warm event (MWE) between ca. 1150 and 1200 CE. In terms of social and cultural reorganization, the MCA period was coincident with the climax of many Mediterranean cultures. During the twelfth century, the medieval Byzantine Empire goes through an important societal expansion, with substantial agricultural productivity, intensive monetary exchange, demographic growth, and its prominent international political situation (Xoplaki et al., 2015).

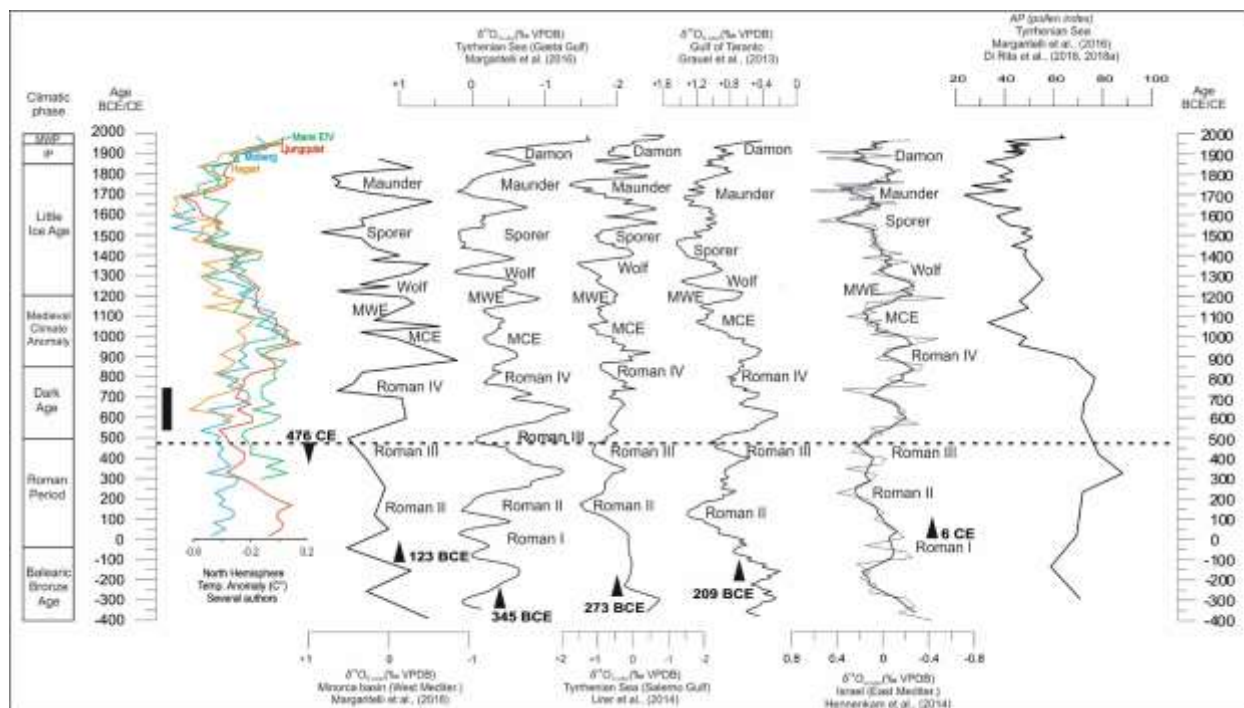


Fig. 1. Comparison in time domain between North Hemisphere mean temperatures reconstruction from different authors [Moberg et al., 2005 (blue curve); Hegerl et al., 2006, 2007 (yellow curve); Mann et al., 2008 (green curve); Ljungqvist et al., 2010 (red curve)],  $\delta^{18}\text{O}_{\text{G.ruber}}$  (% VPDB) of Menorca core (Margaritelli et al.,

2018),  $\delta^{18}\text{OG.ruber}$  (‰ VPDB) of Gulf of Gaeta (Margaritelli et al., 2016),  $\delta^{18}\text{OG.ruber}$  (‰ VPDB) of Gulf of Salerno (Lirer et al., 2013; 2014);  $\delta^{18}\text{OG.ruber}$  (‰ VPDB) of Gulf of Taranto (Grauel et al., 2013),  $\delta^{18}\text{OG.ruber}$  of Israel (Hennenkam et al., 2014) and the Alborean Pollen (AP) index of Margaritelli et al. (2016), Di Rita et al. (2018, 2018a). The acronym MWE corresponds to Medieval Warm Event, and MCE to Medieval Cold. The black arrows with ages represent the ages when this areas becomes part of the Roman Empire. The thick dotted line with associated age 476CE represents the Fall of the Roman Empire. The black vertical bar represents the Justinian Plague. Modified after Margaritelli et al. (2018).

The MCA-LIA transition, between ca. 1200 and 1250 CE, corresponds to the last global scale Rapid Climate Change (RCC) of Mayewski et al. (2004) when the last onset of alpine glacier advance (Holzhauser et al., 2005) is documented. The establishment of colder conditions in the climate system from ca. 1200 CE upwards characterized the entire LIA time interval as documented in north Hemisphere (PAGES 2K Consortium, 2013) and SST (Cisneros et al., 2016) temperature reconstructions and by abrupt oscillation in Mediterranean  $\delta^{18}\text{OG.ruber}$  records (Margaritelli et al., 2018). In particular, four climatic oscillations related to solar activity: Wolf, Spörer, Maunder and Dalton cold events have been indentified (Fig. 2) in the prominent heavy values of Mediterranean  $\delta^{18}\text{OG.ruber}$  records (Lirer et al., 2014; Margaritelli et al., 2016, 2018). This correlation between the  $\delta^{18}\text{OG.ruber}$  signals and solar minima supports the influence of solar forcing on the climate variability in the Mediterranean sea as already introduced in literature (Lirer et al., 2014; Margaritelli et al., 2016, 2018). In addition, as recorded in the previous cold dry event at ca. 1050 CE (MCE), the prominent decline in the forest cover during the Maunder event (Margaritelli, 2016; Di Rita et al., 2018, 2018a) confirms the cold and dry climate condition at regional scale as also documented in the eastern Mediterranean basin by Kaniewski and Van Campo (2014). In addition, a weak North Atlantic Oscillation (NAO) index, associated with Atlantic Blocking event during LIA and in particular during the Maunder cold event (ca. 1700-1800 CE), has been considered by Margaritelli et al. (2016, 2018) and Di Rita et al. (2018, 2018a) as internal climate forcing to explain the changes in planktonic foraminiferal assemblage [the strong abundance increase of the planktonic foraminifera *Globborotalia truncatulinoidea* in the central and western Mediterranean area (Sicily Channel, south, central and north Tyrrhenian Sea, Minorca basin)] and in pollen data, respectively.

Available  $\delta^{18}\text{OG.ruber}$  data for over the last two centuries, and in particular later 1850 CE, show a ca. 1900-1920 CE a further cooling event chronologically associated to Damon solar minimum (Fig. 2). Upwards, a progressive trend vs light values seem to suggest an inversion in regional scale climate vs warm conditions (Lirer et al., 2014; Margaritelli et al., 2016). This warming trend, started after the second industrial revolution, is also confirmed in Sea Surface Temperature reconstruction from Alboran Sea (Niето-Moreno et al., 2013), Minorca basin (Cisneros et al., 2016), Gulf of Lion (Sigre et al., 2016), Taranto Gulf (Versteeght et al., 2007; Grauel et al., 2013) and Aegean Sea (Gogou et al., 2016).

Notwithstanding the oxygen stable isotopic signature, performed on planktonic foraminifera ( $\delta^{18}\text{OG.ruber}$  data), represents a mixing signal of temperature and changes in local seawater isotopic composition (i.e., salinity), and the  $\delta^{18}\text{OG.ruber}$  amplitude oscillation, over the last millennia, are not so prominent as documented during the glacial/interglacial periods, the geographical compilation of all the Mediterranean available  $\delta^{18}\text{OG.ruber}$  data ([paleo metadata Italy-2k.pdf](#)), over the last 3000 years (Alberico et al., 2017), plotted with a 500-years-time windows, allowed us to document a complex response of Mediterranean basin to climate changes where local factor are superimposed to a regional ones.

Closed to the Italy peninsula, between 3000 and 2500 yr BP, the Ionian Sea documents mean  $\delta^{18}\text{OG.ruber}$  values heavier than Tyrrhenian and Adriatic ones (Fig. 2), suggesting warmer temperatures and less salty waters. In addition, local factors (i.e., runoff) might have control the heaviest values documented in the shallow water marine sites of the central Tyrrhenian Sea (Fig. 2). This warm climate condition documented in the Ionian Sea are also well documented in the eastern Mediterranean (Fig. 2), confirming a progressive increase of aridity during this time interval (Kaniewski et al., 2010).

Between 2500 and 2000 yr BP, a turnover in the Italy peninsula climate condition, is documented. In fact, the Tyrrhenian Sea shows an amelioration of the climate condition than the north Ionian and

Adriatic seas (Fig. 2). Conversely, the eastern Mediterranean basin is still the warmest while the south Aegean Sea documents cold climate condition (Fig. 2).

Between 2000 and 1500 yr BP (Roman Period), the surrounding marine areas closed to the Italy peninsula shows an overall regional cold climate condition. As documented by several authors (Lirer et al., 2014; Margaritelli et al., 2016, 2018) this cooling is connected to solar forcing.

Between 1500 and 1000 yr BP (from Dark Age to early part of Medieval Climate Anomaly),  $\delta^{18}\text{O}_{\text{G.ruber}}$  signal shows in the Ionian Sea, Sicily channel and south Tyrrhenian Sea, heavier values than the Adriatic and central-north Tyrrhenian Sea (Fig. 3). Conversely, in the eastern Mediterranean Sea,  $\delta^{18}\text{O}_{\text{G.ruber}}$  data document a further warming (Fig. 3) respect to the Roman Period.

Between 1000 and 500 yr BP (from Medieval Climate Anomaly to early Little Ice Age), all the marine areas closed to the Italy peninsula show overall coldest climate condition (Fig. 3).

Over the last 500 yr BP (from Little Ice Age to the Industrial Period), the  $\delta^{18}\text{O}_{\text{G.ruber}}$  signal documents a further cooling in the Adriatic, Sicily channel and Tyrrhenian Sea, as also in the eastern Mediterranean basin (Fig. 3). Conversely, in the Ionian Sea, stable isotope signal shows a reduction of the cold climate condition (Fig. 3). In this time window, we excluded the  $\delta^{18}\text{O}_{\text{G.ruber}}$  data over the last 150 yr, due to the fact that they are strongly connected to the modern warming phase and to anthropogenic impact.

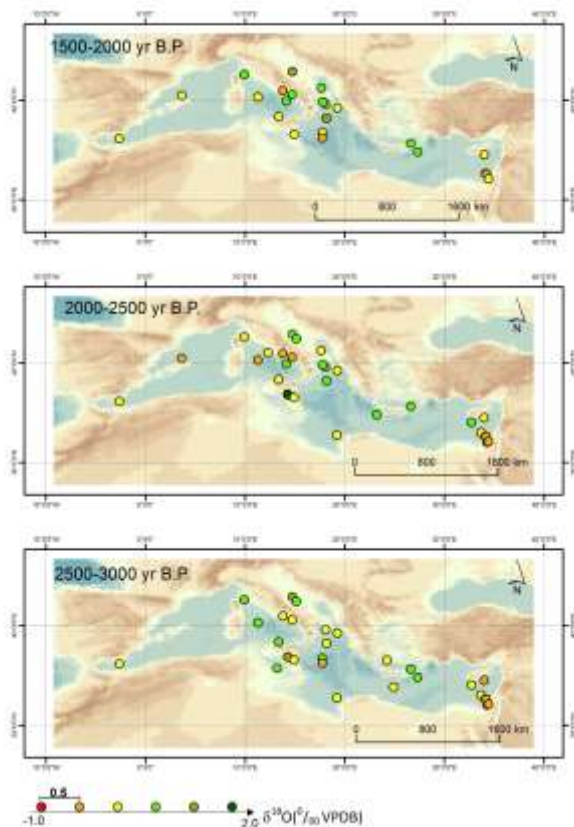


Fig. 2. Geographical distribution of the Mediterranean  $\delta^{18}\text{O}_{\text{G.ruber}}$  data (mean values), between 3000 and 1500 yr BP, plotted with a 500-years-time windows.

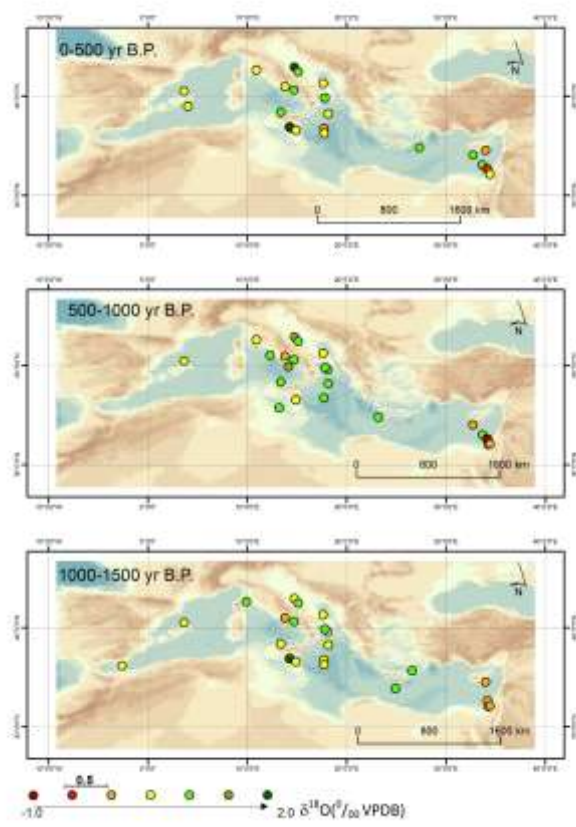


Fig. 3. Geographical distribution of the Mediterranean  $\delta^{18}\text{O}_{\text{G.ruber}}$  data (mean values), between 1500 and 0 yr BP, plotted with a 500-years-time windows.

## References

Alberico, I. Giliberti, D.D. Insinga, P. Petrosino, M. Vallefuoco, F. Lirer, S. Bonomo, A. Cascella, E. Anzalone, R. Barra, E. Marsella, and L. Ferraro, (2017). Marine sediment cores database for the

Mediterranean Basin: a tool for past climatic and environmental studies. *Gruyter Open Geoscience*, 9; 221–239

Cascella A., Bonomo S., Jalali B., Sicre M.-A., Pelosi N., Schmidt S., Lirer F., (accepted for publication, 2019). Paleoclimate history of the last 2700 years in the Southern Adriatic Sea: Coccolithophore evidences. *The Holocene*.

Cisneros M., Cacho I., Frigola J., Canals M., Masqué P., Martrat B., Casado M., Grimalt J., Pena L. D., Margaritelli G. and Lirer F., (2016). Sea surface temperature variability in the central-western Mediterranean Sea during the last 2700 years: a multi-proxy and multi-record approach. *Clim. Past*, 12, 849–869.

Di Rita F., Lirer F., Bonomo S., Cascella A., Ferraro L., Florindo F., Insinga D., Lurcock P., Margaritelli G., Petrosino P., Rettori R., Vallefucio M., Magri D., (2018). Late Holocene forest dynamics in the Gulf of Gaeta (central Mediterranean) in relation to NAO variability and human impact. *Quaternary Science Reviews*, 179; 137-152.

Di Rita F., Fletcher W.J., Aranbarri J., Margaritelli G., Lirer F., Magri D., (2018). Holocene forest dynamics in central and western Mediterranean: periodicity, spatio-temporal patterns and climate influence. *Scientific Reports*, DOI:10.1038/s41598-018-27056-2

Gogou, A., Triantaphyllou, M., Xoplaki, E., Izdebski, A., Parinos, C., Dimiza, M., Bouloubassi, I., Luterbacher, J., Kouli, K., Martrat, B., Toreti, A., Fleitmann, D., Rousakis, G., Kaberi, H., Athanasiou, M., Lykousis, V., (2016). Climate variability and socio-environmental changes in the northern Aegean (NE Mediterranean) during the last 1500 years. *Quat. Sci. Rev.* <http://dx.doi.org/10.1016/j.quascirev.2016.01.009>.

Grauel A.L., Goudeau M.L.S., de Lange G.J., et al. (2013). Climate of the past 2500 years in the Gulf of Taranto, central Mediterranean Sea: a high-resolution climate reconstruction based on  $\delta^{18}O$  and  $\delta^{13}C$  of *Globigerinoides ruber* (white). *The Holocene* 23, 1440–6.

Hegerl, G.C., Crowley, T.J., Hyde, W.T., et al., (2006). Climate sensitivity constrained by temperature reconstructions over the past seven centuries. *Nature* 440, 1029–1032.

Hegerl, G., Crowley, T., Allen, M., et al., (2007). Detection of human influence on a new, validated, 1500 year temperature reconstruction. *J. Clim.* 20, 650–666.

Holzhauser, H., Magny, M. and Zumbuhl, H.J. (2005). Glacier and lake-level variations in west-central Europe over the last 3500 years. *The Holocene* 15: 789-801.

Lirer F., Sprovieri M., Ferraro L., Vallefucio M., Capotondi L., Cascella A., Petrosino P., Insinga D.D., Pelosi N., Tamburrino S., Lubritto C., (2013). Integrated stratigraphy for the Late Quaternary in the eastern Tyrrhenian Sea. *Quaternary International*, 292, 71-85.

Lirer, F., Sprovieri, M., Vallefucio, M., Ferraro, L., Pelosi, N., Giordano, L., Capotondi, L., (2014). Planktonic foraminifera as bio-indicators for monitoring the climatic changes occurred during the last 2000 years in the SE Tyrrhenian Sea. *Integrative Zoology*, 9: 542–554

Ljungqvist, F.C., (2010). A new reconstruction of temperature variability in the extra-tropical Northern Hemisphere during the last two millennia. *Geografiska Ann. Ser. APhys. Geograph.* 92A, 339–351.

Mann, M.E., Zhang, Z., Hughes, M.K., Bradley, R.S., Miller, S.K., Rutherford, S., (2008). Proxy-based reconstructions of hemispheric and global surface temperature variations over the past two millennia. *Proc. Natl. Acad. Sci.* 105, 13252–13257.

Margaritelli G., Cacho I., Català, A., Bellucci L., Lubritto C., Pelosi N., Rettori R., Lirer F., (submitted, 2019). Warm signature of the Roman period in Mediterranean Sea surface temperatures.

Margaritelli G., Cisneros M., Cacho I., Capotondi L., Vallefucio M., Rettori R. and Lirer F., (2018). Climatic variability over the last 3000 years in the central - western Mediterranean Sea (Menorca Basin) detected by planktonic foraminifera and stable isotope records. *Global and Planetary Change*, 169, 179-187.

Margaritelli G., Vallefucio M., Di Rita F., Capotondi L., Bellucci L.G., Insinga D.D., Petrosino P., Bonomo S., Cacho I., Cascella A., Ferraro L., Florindo F., Lubritto C., Lurcock P.C., Magri D., Pelosi N., Rettori R., Lirer F., (2016). Marine response to climate changes during the last five millennia in the central Mediterranean Sea. *Global and Planetary Change*. 142, 53-72.

Mayewski, P.A., Rohling, E., Stager, C., Karlén, W., Maasch, K.A., Meeker, L.D., Meyerson, E.A., Gasse, F., van Kreveld, S., Holmgren, K., Lee-Thorp, J., Rosqvist, G., Rack, F., Staubwasser, M., Schneider, R.R., Steig, E.J., (2004). Holocene climate variability. *Quat. Res.* 62, 243–255.

- Moberg, A., Sonechkin, D.M., Holmgren, K., Datsenko, N.M., Karlén, W., (2005). Highly variable northern hemisphere temperatures reconstructed from low-and high-resolution proxy data. *Nature* 433 (7026), 613–617.
- Nieto-Moreno, V., Martínez-Ruiz, F., Willmott, V., García-Orellana, J., Masqué, P., Sinninghe Damsté, J.S., (2013). Climate conditions in the westernmost Mediterranean over the last two millennia: an integrated biomarker approach. *Org. Geochem.* 55, 1–10.
- Jalali B., Sicre M.-A., Klein V., Schmidt S., Maselli V., Lirer F., Bassetti M.-A., Toucanne S., Jorry S. J., Insinga D., Petrosino P. and Châles F., (2018). Deltaic and coastal sediments as recorders of Mediterranean regional climate and human impact over the past three millennia. *Paleoceanography and Paleoclimatology*, DOI: 10.1029/2017PA003298.
- Katsouras, G., (2009). Paleoclimatographic study of climate variability in the northeastern Mediterranean during the last 20.000 years: a biogeochemical and stable isotopes approach. University of the Aegean, DOI:10.12681/eadd/19333.
- Kaniewski D., Paulissen E., Van Campo E., Weiss H., Otto T., Bretschneider J., Van Lerberghe K., (2010). Late second–early first millennium BC abrupt climate changes in coastal Syria and their possible significance for the history of the Eastern Mediterranean. *Quaternary Research* 74, 207–215
- Kaniewski D. and Van Campo. E., (2014). Pollen-inferred palaeoclimatic patterns in Syria during the Little Ice Age. *Journal of Mediterranean geography. Méditerranée*, 122, 139-144.
- Kontakiotis G., (2016). Late Quaternary paleoenvironmental reconstruction and paleoclimatic implications of the Aegean Sea (eastern Mediterranean) based on paleoceanographic indexes and stable isotopes. *Quaternary International* 401, 28-42
- Rodrigo-Gámiz, M., Martínez-Ruiz, F., Rampen, S.W., Schouten, S., Sinninghe Damsté, J.S., (2014). Sea surface Temperature variations in the western Mediterranean Sea over the last 20 kyr: A dual-organic proxy (UK'37 and LDI) approach. *Paleoceanography*, 29, 87–98
- Sicre, M.A., Jalali, B., Martrat, B., Schmidt, S., Bassetti, M.A., Kallel, N., (2016). Sea surface temperature variability in the North Western Mediterranean Sea (Gulf of Lions) during the Common Era. *Earth Planet. Sci. Lett.* 456, 124–133.
- Versteegh GJM, de Leeuw JW, Taricco C et al. (2007). Temperature and productivity influences on  $U^{K}_{37}$  and their possible relation to solar forcing of the Mediterranean winter. *Geochemistry, Geophysics, Geosystems* 8: Q09005.
- Xoplaki, E., Fleitmann, D., Luterbacher, J., et al., (2015). The Medieval Climate Anomaly and Byzantium: A review of the evidence on climatic fluctuations, economic performance and societal change. *Quat. Sci. Rev.* 136, 229–252.

### **Archivi montani e continentali**

The main goal is to reconstruct the climate variability of the last centuries, mainly related to northern Italy, and provide specific tools for calibrating temperature and precipitation records from pollen and tree rings proxy data. Metadata of all the datasets implemented during the NextData Project are available at: <http://geomatic.disat.unimib.it/dendro> and <http://geomatic.disat.unimib.it/paleodata>. Dendrochronological open access datasets from the Adamello-Presanella and Ortles Cevedale groups are available at:

<https://www.ncdc.noaa.gov/paleo-search/study/19876?siteId=56759> (Val di Fumo – LADE – ITRDB ITAL 041)

<https://www.ncdc.noaa.gov/paleo-search/study/19875?siteId=56758> (Val d’Avio – LADE – ITRDB ITAL040)

<https://www.ncdc.noaa.gov/paleo-search/study/19878?siteId=56761> (Val Presena – LADE – ITRDB ITAL043)

<https://www.ncdc.noaa.gov/paleo-search/study/19877?siteId=56760> (Val Presanella – LADE – ITRDB ITAL042)

<https://www.ncdc.noaa.gov/paleo-search/study/25691?siteId=57757> (Bosco Antico - LADE - ITRDB ITAL050)

<https://www.ncdc.noaa.gov/paleo-search/study/25692?siteId=57758> (Val di Sole - PICE - ITRDB ITAL051)

Other two dataset used in Cerrato et al. 2019 are in preparation for publication on the ITRDB: Val Palù di Vermiglio and Val di Barco.

The database of the main proxy records from ice cores drilled in the mid-latitude glaciers (i.e. European Alps) it is on-line and permitting to reconstruct the variability of the dust transport from North Africa to the Alpine region (<http://geomatica.disat.unimib.it/home/geomatic/idb2>). All the references are listed in the 1.4 and 2.3 deliverables.

The absolute temperature values for the last 3500 years cal BP, mapped using pollen-temperature reconstruction, averaged over 500-years-time windows are presented in Fig. 3. Warmer temperatures are reconstructed for the interval 3500-3000 at Rutor and Crotte Basse sites. Slightly colder temperatures are estimated from 3000 to 2000 years at Rutor and Crotte Basse, while more or less constant temperatures are recorded at Armentarga and Lavarone sites. Part of this interval corresponding to the Iron Age, is marked by glacier expansion in the western Alps (e.g. Badino et al. 2018). Between 2000 and 1500 years cal BP slightly warmer temperatures are estimated for all sites. Slightly colder temperatures are recorded from 1500 years until 500 years cal BP.

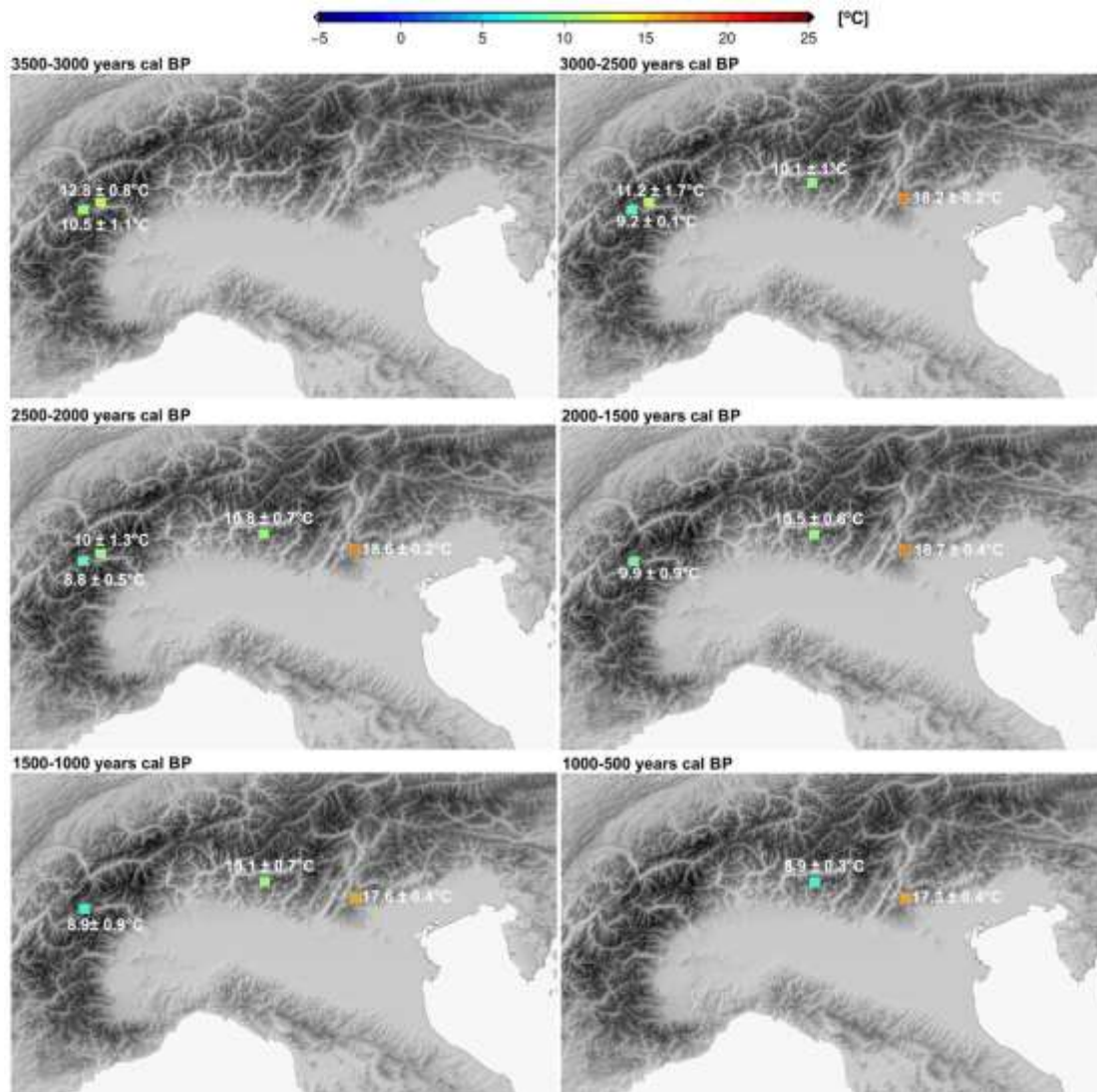


Fig. 4. July temperature (Rutor, Crotte Basse, Armentarga) and summer temperature estimates (Lavarone) in absolute values averaged over 500 years-time windows. The errors represent the standard deviation over the 500-years interval. Reconstructed temperature values were taken from the respective publications: Rutor, Badino et al. 2018; Crotte Basse, Pini et al. 2017; Armentarga, Furlanetto et al. 2018.

High altitude temperatures are also reconstructed with annual resolution for the last five centuries using tree-ring proxy. Specifically, latewood width (LW) measures of one of the most long-living wood sited on the Italian Alps called “Bosco Antico”, were used to estimate the trend of the June-July mean temperature as anomalies and as absolute values at the sampling stand altitude since 1520 AD

finding anomalies variation between  $-2.3$  and  $+1.9$  °C (Fig. 4; Cerrato et al. 2018). These findings add fifty years of temperature reconstruction to previous results (Coppola et al. 2013) that reconstruct the June-August mean temperatures for the Adamello-Presanella massif between 1550 and 2008 (Fig 5). Moreover, highlight also in the northern Italy the loose of sensitivity by *Larix decidua* Mill., as recorded at other sites, caused by the divergence problem, probably due to the ongoing global warming (Coppola et al. 2012, Cerrato et al. 2018). Nevertheless, divergent problem, although ubiquitous, is not recorded at every stand, how it was highlighted in a broad study by Leonelli et al., 2016. In fact, considering only those stand along the Alps that do not shown any divergence between tree-ring proxy and temperatures, the authors were able to reconstruct an High Sensitive To Temperature (HSTT) multispecies chronology that explain around 60% of the temperature variance between 1469 and 2011 (Fig 6). Tree-ring-width investigations result useful also to reconstruct the cyclic outbreaks of a lepidoptera in high-altitude stand. The life cycle of the Larch budmoth is related to the timing of egg hatch and larch needle sprout and was demonstrated that in the last years the rise in temperature bring the optimum belt of the insect to rise along the mountain range before to be completely destroyed, highlighting another effect of the ongoing climate change (Cerrato et al., 2019a)

Moreover, the analysis of the latewood density of the Swiss stone pine (*Pinus cembra* L.), an overlooked species in the alpine range, demonstrate that this parameter can be successfully used as a proxy for a longer window of temperatures with a more than acceptable explained variance not only restricted to the Alpine range but also on a wider area (Cerrato et al., 2019b, Fig. 7)

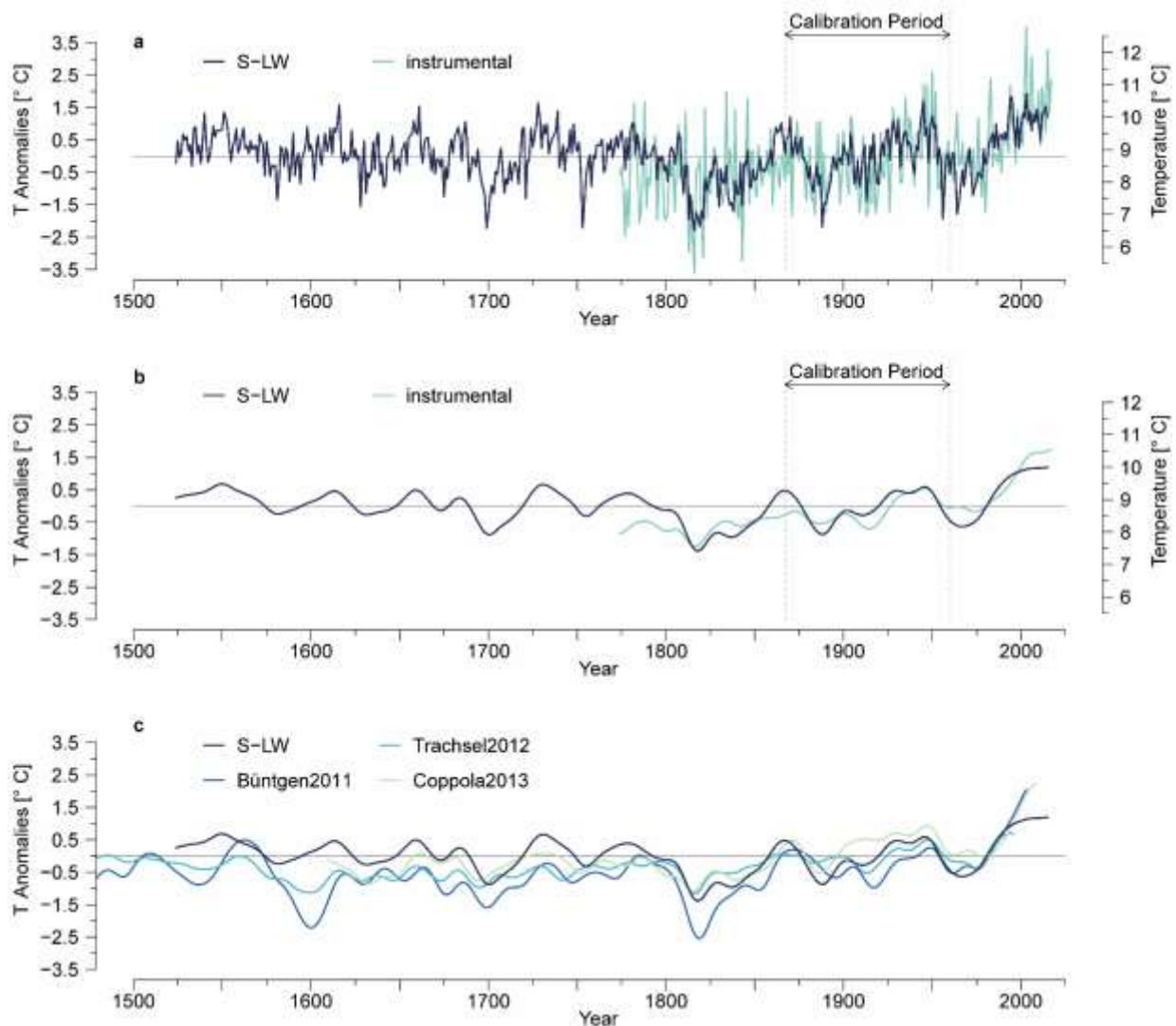


Fig. 5. Yearly Standard Latewood (S-LW) based reconstructed June-July temperature anomalies using the 1867-1960 calibration period (a) and the 31-years Gaussian filtered series (b). Comparison between Bosco



Antico S-LW based reconstructed June-July temperature anomalies and previously published reconstructions (c). (after Cerrato et al., 2018).

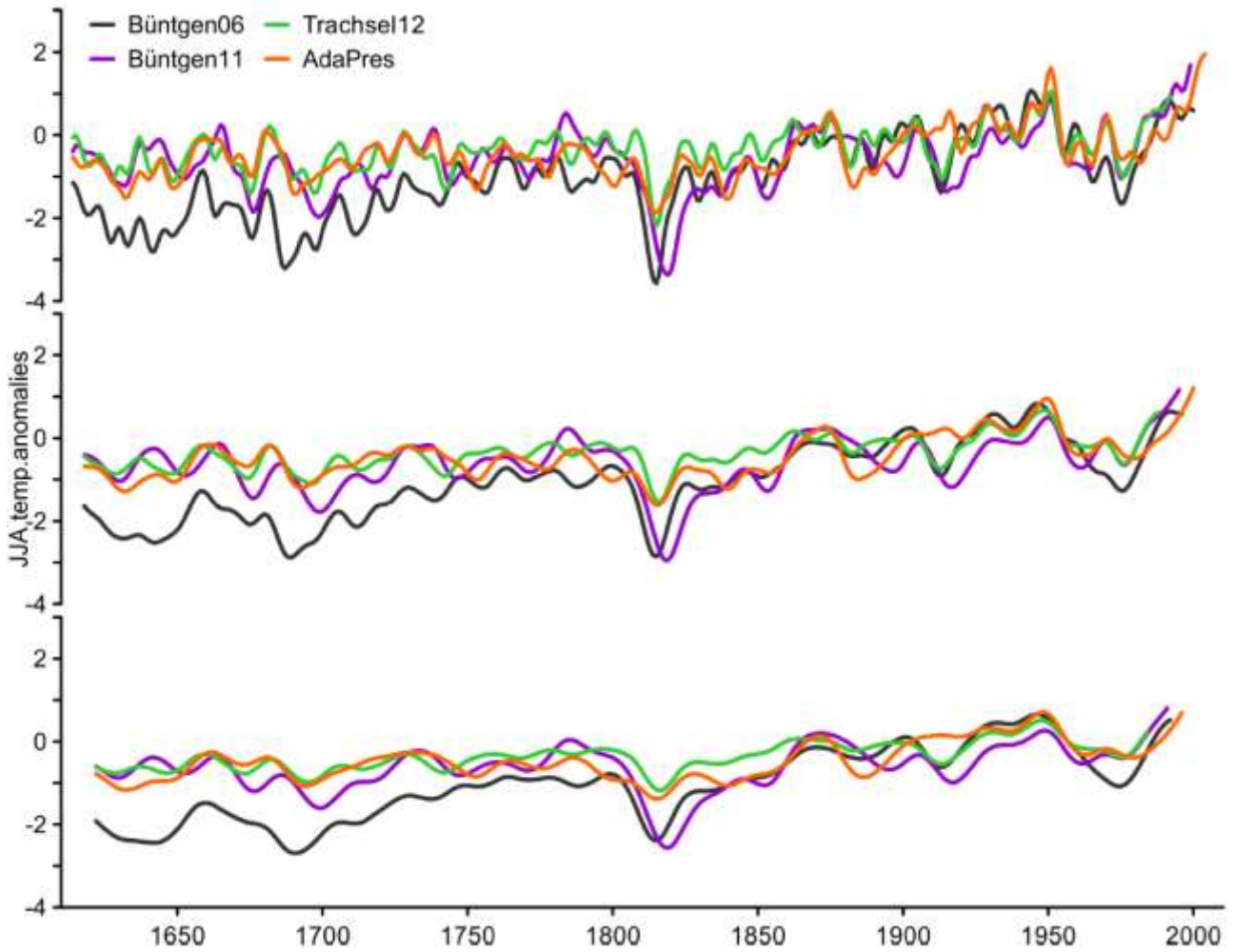


Fig. 6. Comparison between the Adamello-Presarella (AdaPres) reconstruction and the three compared series. All the series were smoothed by means of a Gaussian low-pass filter of 10 (top), 20 (middle) and 30 years (bottom). (Coppola et al., 2013).

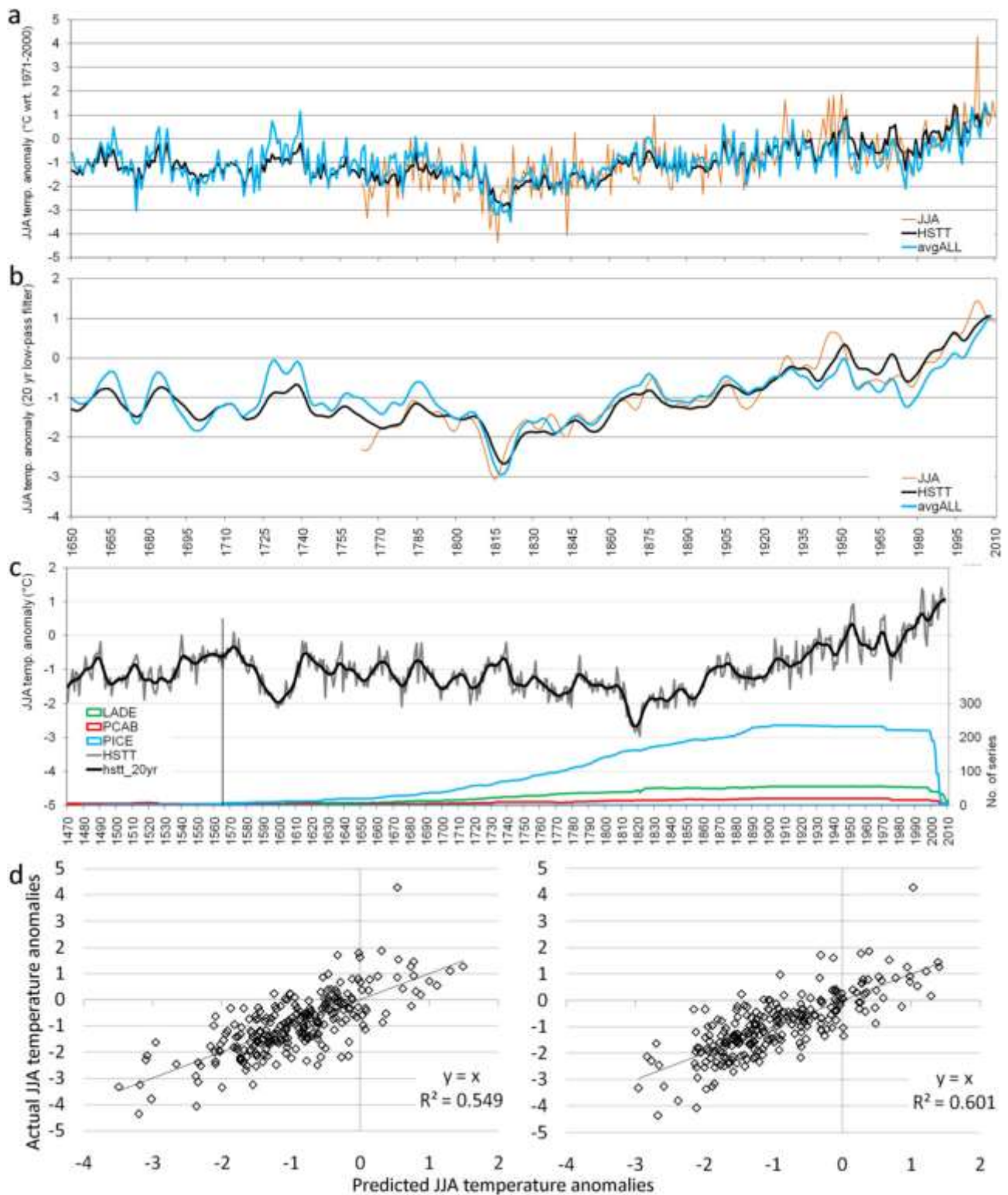


Fig. 7. Reconstruction of June-July-August (JJA) temperature anomalies based on the HSTT and the mean of all chronologies (avgALL)(a). The Gaussian 20-yr. low-pass filtered reconstructions are also reported (b). The HSTT reconstruction and the contribution of the series from different species over time (c): the vertical line in 1566 delimits the older period where the number of series of *P.abies* exceeds the *L.decidua* series. (d) Scatter plot of actual JJA values on predicted JJA temperature anomalies obtained by the avgALL (left) and HSTT (right) models. Regression equations and their respective determination coefficients are also reported (after Leonelli et al., 2016).

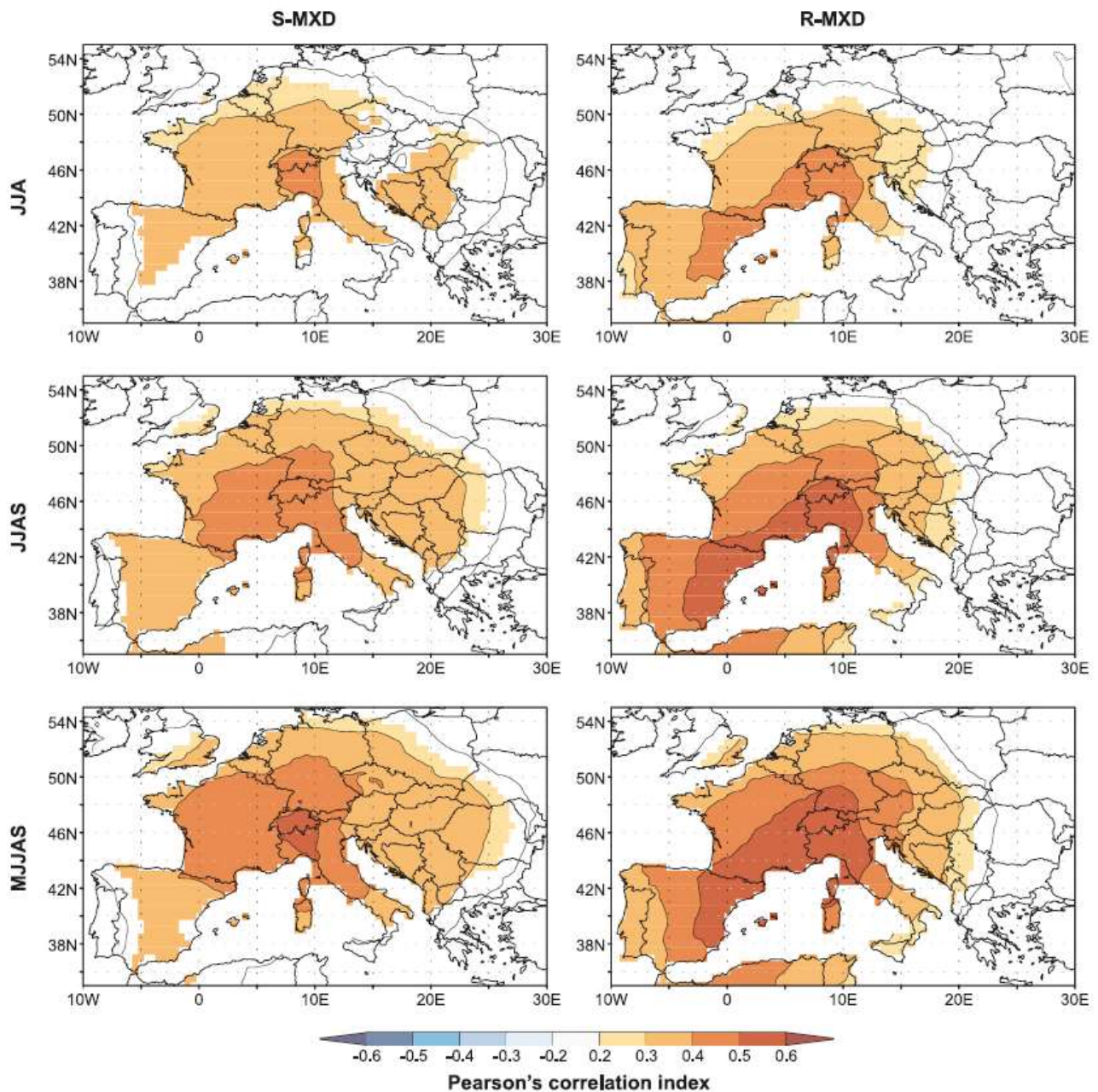


Fig. 8. Pearson's correlation field values between Standard Maximum Latewood density (S-MXD) (left column) or Residual Maximum Latewood density (R-MXD) (right column) and the seasonal mean temperature of the Climate Research Unit (CRU-TS 4.01, Harris et al., 2014) in the 1901–2015 time period. The  $p$ -field threshold was set at  $\alpha=0.01$  (KNMI climate explorer; <http://climexp.kmni.nl>) (after Cerrato et al., 2019).

Temperature reconstructions from tree rings proxies, in the Mediterranean region are less frequent than the reconstruction of precipitation or drought indices, however some efforts have been performed, mainly including sites from mountain environments (under sub-Mediterranean climatic conditions). Even if these reconstructions have temperature as major target, in this environment temperature and precipitation are frequently negatively correlated, especially during summer, and trees respond to high/low temperature and lack/availability of soil moisture. Therefore, the resulting temperature reconstructions often hold precipitation signals. Over a wide northeastern Mediterranean-Balkan region comprising Italy, part of the Italian Alps, the Balkans, Greece and central Romania and Bulgaria, a first late-summer temperature reconstruction was performed using ring-width and MXD data (Trouet, 2014). Based on a tree-based approach similar to the one applied in the Alps, a better performing reconstruction of late-summer temperature has been performed for the Italian Peninsula using only MXD chronologies from the Apennine (Leonelli et al., 2017; deliverable 1.4c). The resulting reconstruction dated back to 1700s and showed very high coherence

with the temperature variability over a wider region comprising Sardinia, Sicily, northern Africa and the Balkans; moreover, it showed also a dipole in precipitation patterns between the northern Balkans and a region comprising the Ireland, Scotland and the southern Scandinavia.

Meteorological extreme event in the Mediterranean area are increasing and one of them give the possibility to sample one of the older pine wood of the Italian peninsula. In fact, after the extreme wind gust occurred in March 2015, the working group had the possibility to take sample from the "Versiliana" park sited in Forte dei Marmi, Tuscany. The samples belong to trees up to two hundreds years old and potentially will give us the possibility to reconstruct drought stress in this area of the Mediterranean with annual resolution (Coppola et al. *in preparation*)

Multi-proxy approaches in past climate reconstructions need in the first steps a selection of appropriate climate sensitive records and a deep evaluation of their inner variability. Moreover, as regards tree rings and pollen-stratigraphical records, they typically cover different time lengths and show different time resolutions. In order to assess the relationships between the variability of these two proxy records it is therefore restrict the comparison between two proxies over a selected common period (usually the most recent) and perform an adaptation of the annually-resolved resolution of the tree rings to the generally lower and variable resolution of the pollen-stratigraphical records.

Main results provide comparison between two summer temperature reconstructions derived from these two proxy records was performed in the central sector of the Italian Alps by selecting an area of approximately 150 km of diameter, comprising tree-ring series of European larch (*Larix decidua* Mill.), Norway spruce (*Picea abies* Karst.) and Swiss stone pine (*Pinus cembra* L.) from 42 sites located in five mountain groups - namely the Silvretta Group (Switzerland), the Ötztaler-Venoste Alps (Austria, Italy), the Bernina Group (Switzerland, Italy), the Ortles-Cevedale Group (Italy) and the Adamello-Presanella Group (Italy) and the pollen-stratigraphical record from the Lavarone Lake (Trento), located at 1115 m asl. The entire methodology is well explained in the Deliverable 1.4B. Both the tree-ring (Leonelli et al., 2016) and the pollen-inferred reconstructions were calibrated using the modelled site specific temperatures from an improved version of the dataset of Brunetti et al. (2006). The independently obtained summer temperature reconstructions, after adapting the tree-ring series to the time resolution of the pollen series, showed a good correlation ( $r^2=0.6$ ) over the common period 1803-2003 (Deliverable 1.4a).

Mid-latitude glaciers provide shorter ice core records than polar glaciers: indeed, the longest records only cover a couple of centuries till one millennia (Bohleber et al., 2018, Gabrielli et al., 2016, Schwerzmann et al., 2006; 1995; Prunkner et al., 2000). In effect to avoid disturbances, only records from high altitude glaciers, where the risk of melting is low, can provide environmental and climatic proxy data (Maggi et al., 2006). Although restricted to a regional scale and to relatively short timescales, glaciers in the European Alps can be very useful natural history archives. Unfortunately, mid-latitude glaciers with the appropriate characteristics for preserving glacio-chemical and glacio-meteorological records are quite scarce. In the European Alps only few areas above the 4000 m a.s.l., around the Mont Blanc, Monte Rosa Massifs, and Ortles-Cevedale Group, representing the uppermost part of the accumulation zone of mountain glaciers, have been identified as sites potentially suitable for ice-core studies (<http://geomatica.disat.unimib.it/home/geomatic/idb2>; Fig. 8).

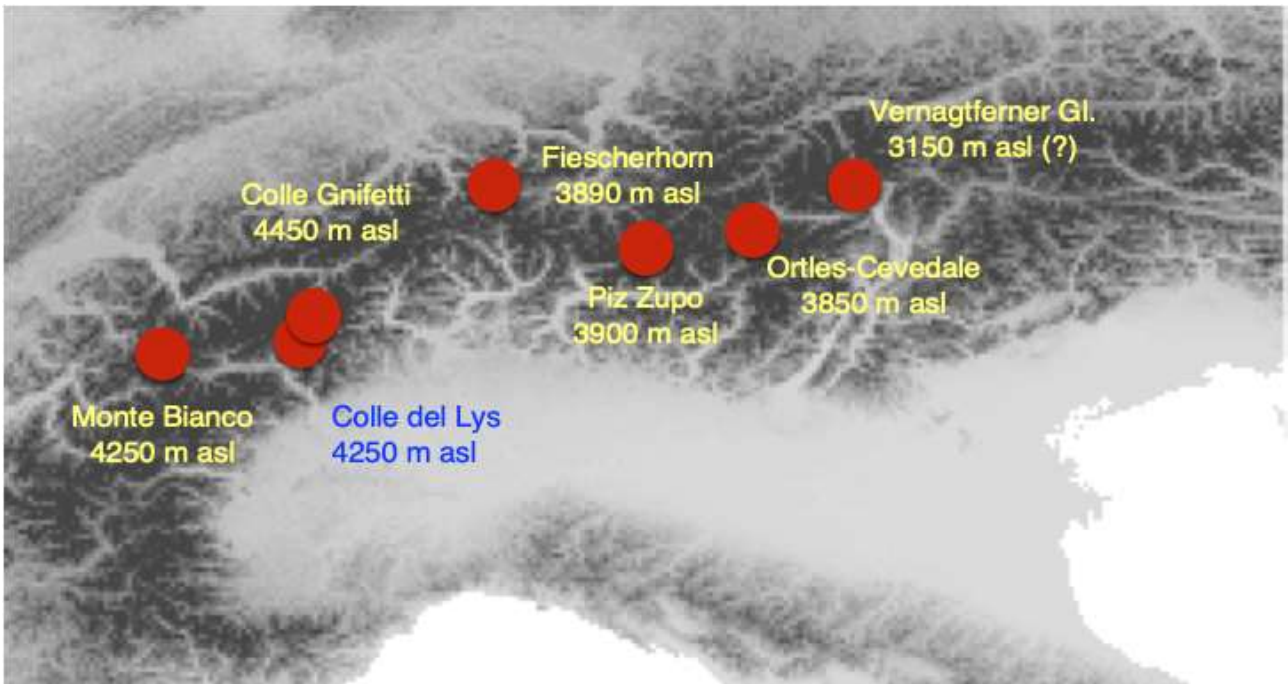


Fig. 9. Map of the main drilling site in European Alps.

Dust transport towards the Mediterranean area and Europe is primarily associated with the occurrence of southerly flows ahead of synoptic frontal systems traveling eastward across the Mediterranean or originating in North Africa and moving north-eastward (Di Mauro et al., 2018; Thevenon et al., 2011). In addition, the synoptic situations favoring the transport of Saharan dust plumes towards western Europe are frequently associated with precipitation over the Alps, where dust scavenging originates colored layers that may be preserved in glacial masses. It is therefore important to identify such “Saharan dust events” (hereafter SDE) as stratigraphic markers for ice-core dating; it must be noted that in this context the generic term "Saharan" refers mainly to the regions of North Africa (Morocco, Algeria, Tunisia and Libya), which are considered the dominant sources of dust in this part of Europe (Thevenon et al., 2011;).

The dust concentration (both, microparticles and Calcium records), mainly related to the transport from North Africa seem to have a general feature along the Alpine area. In the first half of the XX century, the dust reaching important levels due to the general transport from the North Africa. More concentrated seem to be for last 2 decades and beginning of XXI century. In the contrary the middle of XX century the level seems to be lower, especially in the total dust. In reality exists some difficulty to interpret these data, because the transport from North Africa across the Mediterranean use different baric mechanisms (Fig. 10).

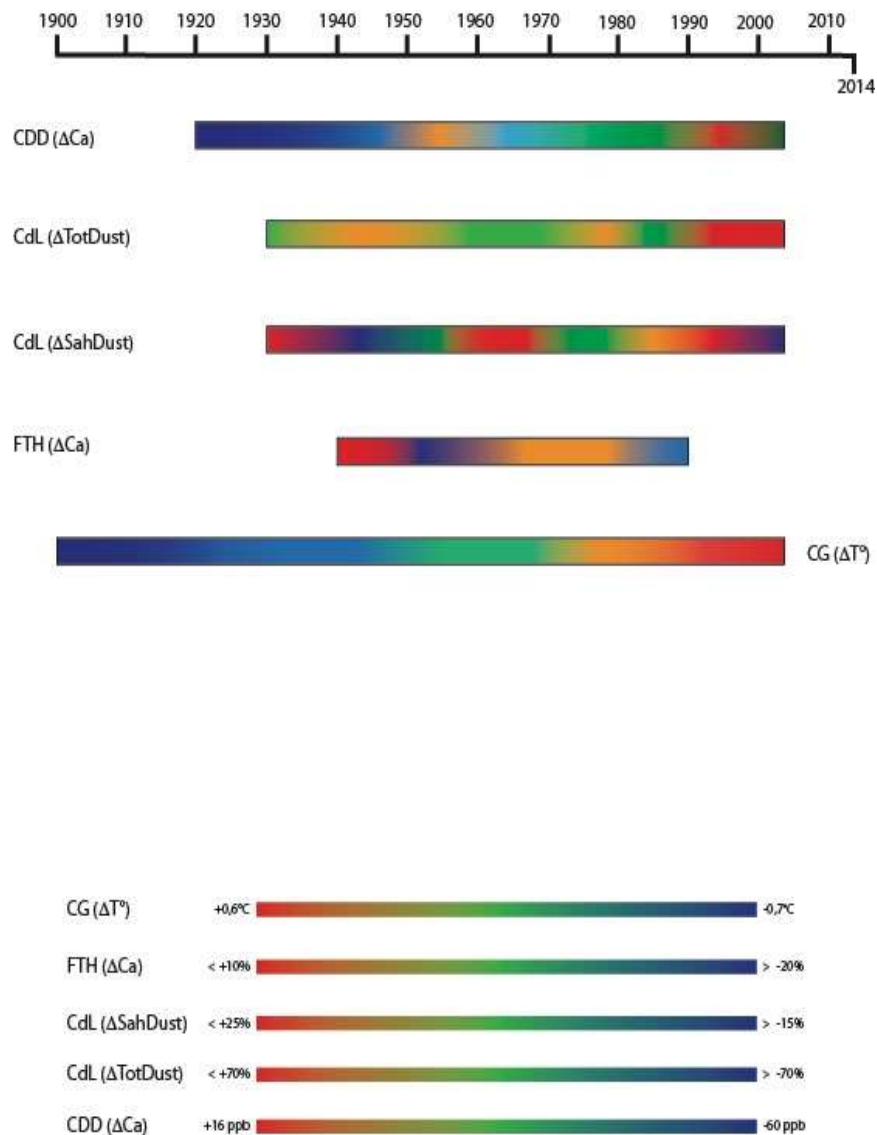


Fig. 10. Variability of the mineral dust transport on the Alpine area from the main records. (CDD=Col du Dome, Monte Bianco; CdL= Colle el Lys, Monte Rosa; FTH= Fiescherhorn, Austria; CG= Colle Gnifetti, Monte Rosa).

## References

- Badino, F., Ravazzi, C., Vallè, F., Pini, R., Aceti, E., Brunetti, M., Champvillair, E., Maggi, V., Maspero, F., Perego, R., Orombelli, G., (2018). 8800 years of high-altitude vegetation and climate history at the Rutor Glacier forefield, Italian Alps. Evidence of middle Holocene timberline rise and glacier contraction. *Quaternary Science Reviews* 185, 41–68.
- Bohleber, P., Erhardt, T., Spaulding, N., Hoffmann, H., Fischer, H., and Mayewski, P., (2018). Temperature and mineral dust variability recorded in two low-accumulation Alpine ice cores over the last millennium, *Clim. Past*, 14, 21-37, <https://doi.org/10.5194/cp-14-21-2018>, 2018.
- Brunetti, M., Maugeri, M., Monti, F., and Nanni, T., (2006). Temperature and precipitation variability in Italy in the last two centuries from homogenised instrumental time series, *Int. J. Climatol.*, 26, 345–381.
- Cerrato R., Salvatore M.C., Brunetti M., Coppola A. & Baroni C. (2018). Dendroclimatic relevance of “Bosco Antico”, the most ancient living European larch wood in the Southern Rhaetian Alps (Italy). *Geografia Fisica e Dinamica Quaternaria*, 41 (1), 35–49.
- Cerrato R., Cherubini P., Büntgen U., Coppola A., Salvatore M. & Baroni C. (2019a). Tree-ring-based reconstruction of larch budmoth outbreaks in the Central Italian Alps since 1774 CE. *iForest - Biogeosciences and Forestry*, 12 (3), 289–296.

Cerrato R., Salvatore M.C., Gunnarson B.E., Linderholm H.W., Carturan L., Brunetti M., De Blasi F. & Baroni C. (2019b). A *Pinus cembra* L. tree-ring record for late spring to late summer temperature in the Rhaetian Alps, Italy. *Dendrochronologia*, 53, 22–31.

Coppola A., Leonelli G., Salvatore M.C., Pelfini M. & Baroni C. (2012). Weakening climatic signal since mid-20th century in European larch tree-ring chronologies at different altitudes from the Adamello-Presanella Massif (Italian Alps). *Quaternary Research*, 77 (3), 344–354.

Coppola A., Leonelli G., Salvatore M.C., Pelfini M. & Baroni C. (2013). Tree-ring- Based summer mean temperature variations in the Adamello-Presanella Group (Italian Central Alps), 1610-2008 AD. *Climate of the Past*, 9 (1), 211–221

Di Mauro, B., Garzonio, R., Rossini, M., Filippa, G., Pogliotti, P., Galvagno, M., Morra di Cella, U., Migliavacca, M., Baccolo, G., Clemenza, M., Delmonte, B., Maggi, V., Dumont, M., Tuzet, F., Lafaysse, M., Morin, S., Cremonese, E., and Colombo, R., (2019). Saharan dust events in the European Alps: role in snowmelt and geochemical characterization, *The Cryosphere*, 13, 1147-1165, <https://doi.org/10.5194/tc-13-1147-2019>.

Gabrielli, P., Barbante, C., Bertagna, G., Bertó, M., Binder, D., Carton, A., Carturan, L., Cazorzi, F., Cozzi, G., Dalla Fontana, G., Davis, M., De Blasi, F., Dinale, R., Dragà, G., Dreossi, G., Festi, D., Frezzotti, M., Gabrieli, J., Galos, S. P., Ginot, P., Heidenwolf, P., Jenk, T. M., Kehrwald, N., Kenny, D., Magand, O., Mair, V., Mikhalenko, V., Lin, P. N., Oeggli, K., Piffer, G., Rinaldi, M., Schotterer, U., Schwikowski, M., Seppi, R., Spolaor, A., Stenni, B., Tonidandel, D., Uglietti, C., Zagorodnov, V., Zanoner, T., and Zennaro, P., (2016). Age of the Mt. Ortles ice cores, the Tyrolean Iceman and glaciation of the highest summit of South Tyrol since the Northern Hemisphere Climatic Optimum, *The Cryosphere*, 10, 2779–2797, <https://doi.org/10.5194/tc-10-2779-2016>.

Leonelli, G., Battipaglia, G., Cherubini, P., Saurer, M., Siegwolf, R.T.W., Maugeri, M., Stenni, B., Fusco, S., Maggi, V. and Pelfini, M., (2017). *Larix decidua*  $\delta^{18}\text{O}$  tree-ring cellulose mainly reflects the isotopic signature of winter snow in a high-altitude glacial valley of the European Alps. *Science of the Total Environment*, 579: 230-237.

Leonelli G., Coppola A., Baroni C., Salvatore M.C., Maugeri M., Brunetti M. & Pelfini M. (2016). Multispecies dendroclimatic reconstructions of summer temperature in the European Alps enhanced by trees highly sensitive to temperature. *Climatic Change*, 137 (1–2), 275–291.

Leonelli G., Coppola A., Salvatore M.C., Baroni C., Battipaglia G., Gentilesca T., Ripullone F., Borghetti M., Conte E., Tognetti R., Marchetti M., Lombardi F., Brunetti M., Maugeri M., Pelfini M., Cherubini P., Provenzale A., Maggi V. (2017). Climate signals in a multispecies tree-ring network from central and southern Italy and reconstruction of the late summer temperatures since the early 1700s. *Climate of the Past*, 13, 1451-1471, doi: 10.5194/cp-13-1451-201

Maggi, V., Villa, S., Finizio, A., Delmonte, B., Casati, P., Marino, F., (2006). Variability of anthropogenic and natural compounds in high altitude-high accumulation alpine glaciers. *Hydrobiologia* 562, 43-56.

Preunkert, S., Wagenbach, D., Legrand, L., and Vincent, C., (2000). Col du Dôme (Mt Blanc Massif, French Alps) suitability for ice-core studies in relation with past atmospheric chemistry over Europe, *Tellus*, 52B, 993–1012.

Schwerzmann, A., Funk, M., Blatter, H., Lüthi, M., Schwikowski, M., and Palmer, A., (2006). A method to reconstruct past accumulation rates in alpine firn regions: A study on Fiescherhorn, Swiss Alps, *J. Geophys. Res.-Earth*, 111, F01014, <https://doi.org/10.1029/2005JF000283>.

Thevenon, F., Guédron, S., Chiaradia, M., Loizeau, J., & Poté, J. (2011). (Pre-) historic changes in natural and anthropogenic heavy metals deposition inferred from two contrasting Swiss alpine lakes. *Quaternary Science Reviews*, 30(1–2), 224–233. <https://doi.org/10.1016/j.quascirev.2010.10.013>

Trouet, V., (2014). A tree-ring based late summer temperature reconstruction (AD 1675–1980) for the northeastern Mediterranean, *Radiocarbon*, 56, S69–S78, [https://doi.org/10.2458/azu\\_rc.56.18323](https://doi.org/10.2458/azu_rc.56.18323).